

10<sup>th</sup> U.S. National Combustion Meeting  
Organized by the Eastern States Section of the Combustion Institute  
April 23–26, 2017  
College Park, Maryland

## A comparison of combustion dynamics for multiple 7-point lean direct injection combustor configurations

*Kathleen M. Tacina<sup>1,\*</sup> and Yolanda R. Hicks<sup>1</sup>*

<sup>1</sup>*Engine Combustion Branch, NASA Glenn Research Center, Cleveland, OH*

*\*Corresponding author: kathleen.m.tacina@nasa.gov*

**Abstract:** The combustion dynamics of two 7-point lean direct injection (LDI) combustor configurations are compared. This 7-point LDI configuration has a circular cross section, with a center (“pilot”) fuel-air mixer surrounded by six outer (“main”) fuel-air mixers. Each fuel-air mixer consists of an axial air swirler followed by a converging-diverging venturi. A simplex fuel injector is inserted through the center of the air swirler, with the fuel injector tip located near the venturi throat. All 7 fuel-air mixers are identical except for the swirler blade angle. In the ‘all-60’ configuration, the swirler blade angle was 60° for all fuel-air mixers. In the ‘45-60’ configuration, the swirler blade angle was 60° on the center and 45° on the outer fuel-air mixers. Testing was done in a 5-atm flame tube with inlet air temperatures from 630 to 830 F and equivalence ratios from 0.2 to 0.7. Combustion dynamics were measured using a cooled PCB pressure transducer flush-mounted in the wall of the combustor test section. Both configurations had large pressure fluctuations (> 2 psi peak-peak) near 730 Hz, the quarter-wave frequency. The all-60 configuration also had large pressure fluctuations near 1170 Hz; the 45-60 configuration did not. The 45-60 configuration had large pressure fluctuations near 480 Hz; the all-60 configuration did not.

**Keywords:** *combustion dynamics, lean direct injection*

### 1. Introduction

To reduce aircraft engine emissions of nitrogen oxides (NOx), NASA Glenn has developed multi-element lean direct injection (LDI) combustion technology[1–3]. As the name implies, in LDI the combustor operates fuel-lean without a rich front end: all of the combustion air not used for liner cooling enters through the combustor dome. To prevent local near-stoichiometric regions that produce high NOx emissions, LDI relies on rapid and uniform fuel/air mixing. To promote this rapid mixing, several small fuel-air mixers replace one traditionally-sized fuel-air mixer.

The 7-point swirl-venturi LDI configurations described in this paper were designed (1) to conduct fundamental studies of fuel-air mixing and (2) to serve as a test bed for passive and active combustion control concepts. Compared to similar LDI designs[4–7], the 7-point configurations have weaker (or nonexistent) recirculation zones and higher combustion dynamics. The reason for the decreased recirculation seems to be the smaller element-to-element spacing in the 7-point configurations. The decreased recirculation and increased combustion dynamics make the 7-point configurations a poor choice for a practical combustor. However, it does make it a nice testbed for testing passive and active combustion control concepts.

This paper describes combustion dynamics for two 7-point configurations.



Figure 1: SV-LDI: (a) a single SV-LDI fuel-air mixer and (b) the 7-point SV-LDI configuration.

## 2. Hardware and Experimental Facilities

### 2.1 LDI Configurations

Each of the fuel-air mixers in LDI is relatively simple. As shown in Fig. 1a, a single swirl-venturi LDI (SV-LDI) fuel-air mixer consists of a fuel injector and an air passage with an axial air swirler followed by a converging-diverging venturi section. The fuel injector is inserted through the center of the air swirler, with the tip typically located at or just upstream of the venturi throat.

There are slight variations in the geometry of each SV-LDI fuel-air mixer. For the experiments reported here, the nominal fuel-air mixer size is 1-in. The air swirler is 6-bladed with a hub diameter of 0.34-in and a blade diameter of 0.8725-in. The venturi throat diameter is 0.5-in and the throat length is 0.061-in. The fuel injector is a simplex nozzle, which produces a hollow-cone spray; the flow number  $FN_{US}$  is 0.7 and the cone angle is approximately  $70^\circ$ .

Results from two SV-LDI configurations are reported here. The configurations are identical except for swirler blade angle. The 'all-60' configuration has a swirler blade angle of  $60^\circ$ . The 45-60 configuration has a swirler blade angle of  $45^\circ$  on the outer 6 main swirlers and  $60^\circ$  on the center pilot swirler.

### 2.2 Experimental Facility

All testing was done at NASA Glenn Research Center's Combustion and Dynamics Facility (CDF). The CDF is orientated vertically, with the flow going down. It can supply noninitiated air preheated to 800 F at air flow rates up to 0.8 lbm/sec and pressures up to 75 psia. The combustor test section is water-cooled and has a circular cross-section nominally 3-in in diameter. Before the combustion products are exhausted, they are cooled using water spray. The first spray nozzle is approximately 10.5-in downstream of the combustor dome.

Dynamic pressure fluctuations were measured using a cooled, PCB sensor flush-mounted on the combustor wall. Data was recorded using a Data Translation DT9841-sb high-speed data acquisition system, typically at a 60 kHz data acquisition rate for between 30 and 120 seconds. Steady-state data was recorded using Labview.

## 3. Data Analysis

The dynamic pressure fluctuations were processed as follows. First, the rolling mean over 0.1 sec was calculated and subtracted from the dynamic pressure signal (Fig. 2, left two plots). Then, the

## Sub Topic: Internal Combustion Engines and Gas Turbines

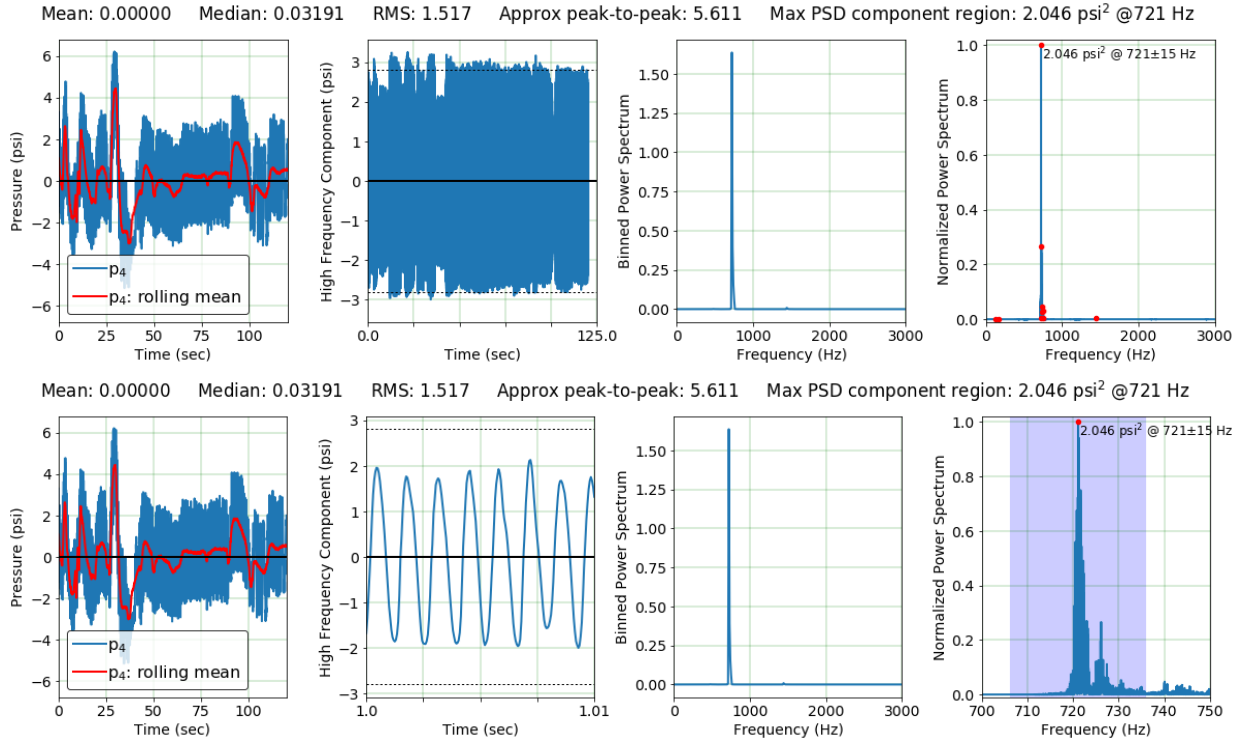


Figure 2: Example of data analysis for the 45-60 configuration. Test conditions are: inlet temperature 750 F, inlet pressure 63 psia, equivalence ratio 0.61 with the center fuel-air mixer about 30% richer than the outer fuel-air mixers, and cold flow reference velocity 41 ft/s.

power spectrum<sup>1</sup> was calculated using the real fourier transform with essentially all of the original data (i.e, Welch's method or Bartlett's method were *not* used).

The power spectrum results were visualized in three ways. First, the power spectrum components were summed into 10-Hz bins; see the second-from-right plots in Figure 2. Second, the power spectrum components were normalized by the peak component and plotted in the right-most plots in Figure 2. Third, the peaks in the power spectrum were found using a peak-finding algorithm and the components within  $\pm 15$  Hz of this peak were summed together.

It is this last method that is used for the later figures in this paper.

## 4. Results and Discussion

### 4.1 Results

Figure 3 shows the rms of the pressure fluctuations as a function of the bulk cold flow and bulk hot gas velocities. Also plotted are pressure fluctuations for nonreacting cases. For the nonreacting cases, the rms seems to be function of bulk velocity, as would be expected. Some of the reacting cases also seem to fall on the same bulk hot gas velocity-rms curve. These points are labeled “low rms” cases. For other reacting cases, the rms pressure fluctuations fall significantly above this

<sup>1</sup>Note: The power spectrum can be defined in several ways. In this paper, the power spectrum is calculated so that the sum of the components of the power spectrum is equal to the variance, i.e., the rms<sup>2</sup>.

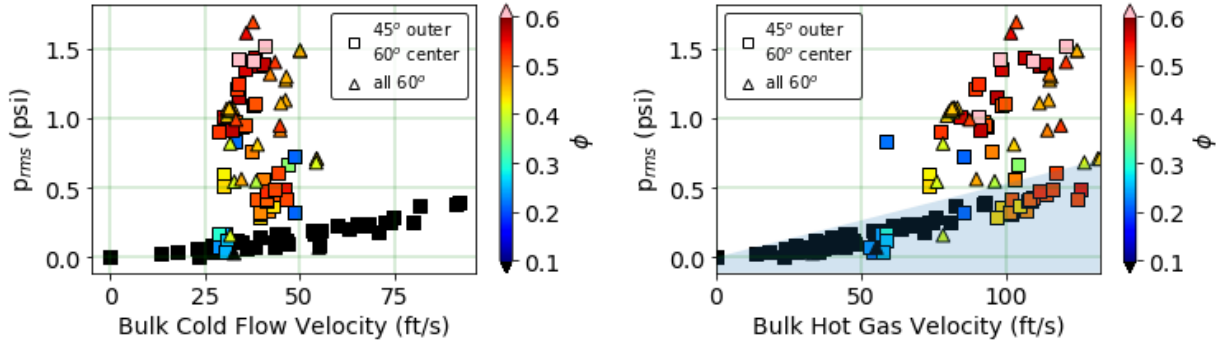


Figure 3: RMS of pressure fluctuations as a function of (left) bulk cold flow velocity and (right) bulk hot gas velocity. The "low rms" region is indicated by blue shading.

curve; these are labeled "high rms" cases.

The peaks in the power spectrum for the low and high rms cases are compared in Fig. 4-5. The top row of Fig. 4 shows that peaks in the power spectrum occur in the same frequency ranges for both the high and low rms cases. However, Fig. 5 shows one difference: for the 45-60 configuration, the largest peak is near 1200 Hz only for low rms cases.

Comparing the power spectrum for the 45-60 and all-60 configurations shows that both configurations have large peaks near 730 Hz. Both configurations also have large peaks near 480 Hz and 1175 Hz. However, for the 45-60 configuration, the peaks near 480 Hz are larger than those near 1175 Hz; for the all-60 configuration, the reverse is true.

## 4.2 Discussion

For some frequencies, the mechanism responsible for the peaks can be identified. The 730-Hz frequency is probably an acoustic mode: it is near the quarter wave frequency of the about 10.5-in long cylinder from the combustor dome to the first water spray bar. The peaks near 730-Hz are typically not very sharp — see the lower-right plot in Fig. 2 — which would be expected for a boundary defined by a water spray.

The 0.25 psi<sup>2</sup> peaks near 60 Hz indicate the nearness of lean blowout: in both of these cases, a flameout occurred.

The small-magnitude frequency peaks at 1,500 Hz and above could be caused by a precessing vortex core (PVC). Previous results from a single-element LDI configuration indicate that the frequency of the PVC with 60° swirlers depends only on bulk cold flow velocity (i.e., constant Strouhal number). Assuming that this Strouhal number is the same for the 7-point configurations, the PVC frequency would range from 1,250 to 2,500 Hz.

The origin of the frequency components near 480 Hz and 1175 Hz is not known. It is possible that the near 480 Hz peak could be a beat frequency. It is true that 480 Hz is larger than the 405 Hz difference between 730 Hz and 1175 Hz. However, examining the individual cases where peaks at all three frequencies are present shows that the difference is often much smaller. For example, in one case the near-730 Hz frequency is at 717 Hz, the near-480 Hz frequency is at 470 Hz, and the near-1175 Hz frequency is at 1186 Hz. In this case, the difference (1186-717 Hz) is only 1 Hz different than the measured peak at 470 Hz. In addition, note that the peaks are typically diffuse,

## Sub Topic: Internal Combustion Engines and Gas Turbines

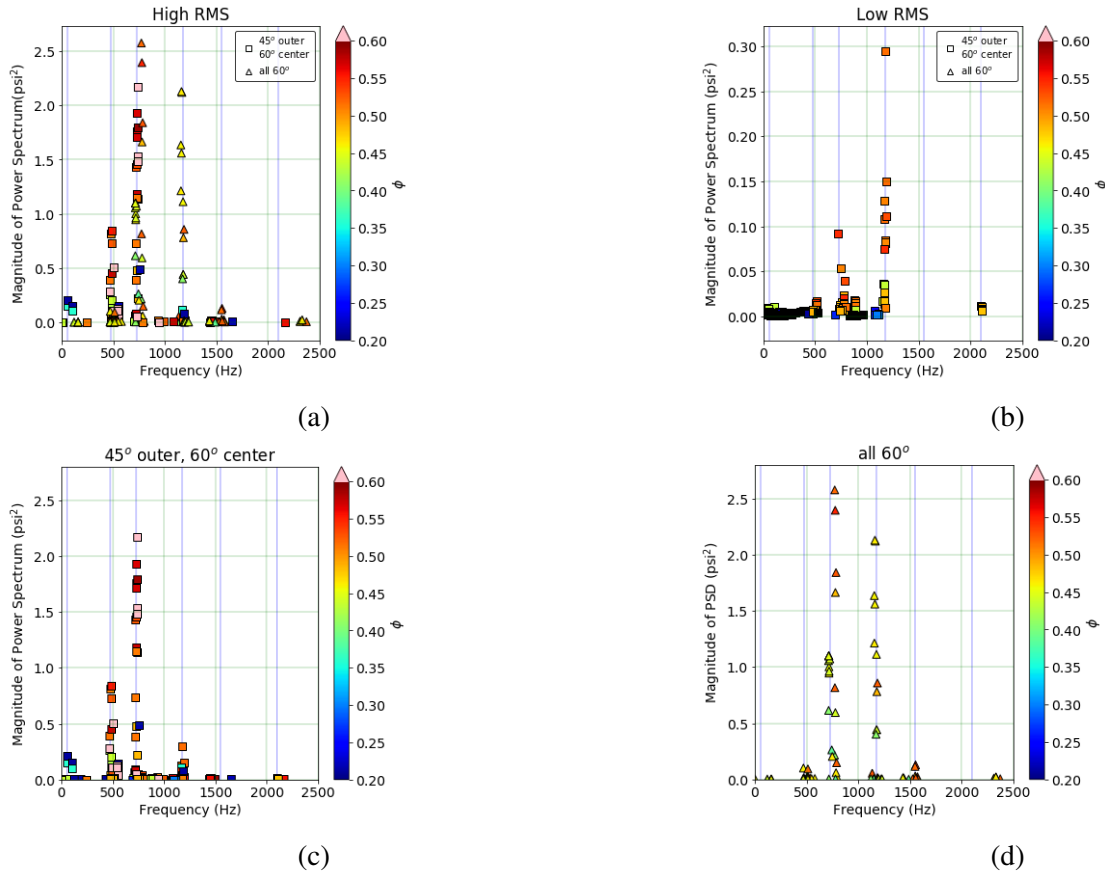


Figure 4: Magnitude of power spectrum as a function of frequency for 30-Hz regions where the power spectrum is at least  $0.001 \text{ psi}^2$ .

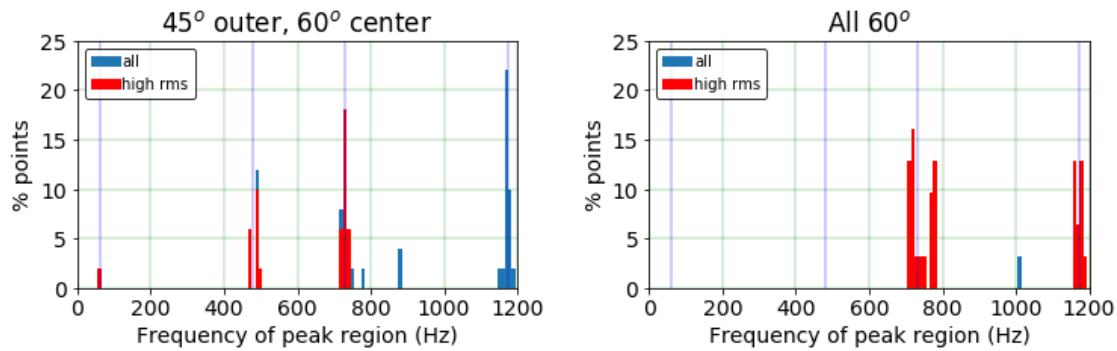


Figure 5: Frequency of peak power spectrum (30-Hz region)

## Sub Topic: Internal Combustion Engines and Gas Turbines

not narrow. Thus, it is possible that the near-480 Hz peak is caused by interaction of some acoustic phenomena near 1175 Hz and the quarter-wave acoustic mode near 730 Hz.

### 5. Summary

The combustion dynamics of two 7-point lean direct injection (LDI) combustor configurations are compared. Both configurations had large pressure fluctuations (> 2 psi peak-peak) near 730 Hz, the quarter-wave frequency. The all-60 configuration also had large pressure fluctuations near 1170 Hz; the 45-60 configuration did not. The 45-60 configuration had large pressure fluctuations near 480 Hz; the all-60 configuration did not.

### 6. Acknowledgements

This research was funded by the Transformational Tools and Technologies project of NASA Aeronautics.

### References

- [1] R. Tacina, P. Lee, and C. Wey, A Lean-Direct-Injection Combustor Using a 9 Point Swirl-Venturi Fuel Injector, ISABE-2005-1106 Report No., 2005.
- [2] R. Tacina, C. Wey, P. Laing, and A. Mansour, A Low-NOx Lean-Direct Injection, MultiPoint Integrated Module Combustor Concept for Advanced Aircraft Gas Turbines, NASA/TM-2002-211347 Report No., 2005.
- [3] R. Tacina, C.-P. Mao, and C. Wey, Experimental Investigation of a Multiplex Fuel Injector Module with Discrete Jet Swirlers for Low Emissions Combustors, AIAA-2004-0135 Report No., 2004.
- [4] C. M. Heath, Y. R. Hicks, R. C. Anderson, and R. J. Locke, Optical Characterization of a Multipoint Lean Direct Injector for Gas Turbine Combustors :Velocity and Fuel Drop Size Measurements, GT2010-22960 Report No., 2010.
- [5] Y. R. Hicks, C. M. Heath, R. C. Anderson, and K. M. Tacina, Investigations of a combustor using a 9-point swirl-venturi fuel injector: recent experimental results. ISABE-2011-1106 Report No., 2011.
- [6] K. Ajmani, CFD Analysis of Emissions for a Candidate N+3 Combustor, ISABE-2015-20245 Report No., 2015.
- [7] W. A. Acosta and C. T. Chang, Experimental Combustion Dynamics Behavior of a Multi-Element Lean Direct Injection (LDI) Gas Turbine Combustor, AIAA 2016-4589 Report No., 2016.